Journal of Electrochemical Science and Technology
Vol. 2, No. 3, 2011, 157-162
DOI:10.5229/JECST.2011.2.3.157

Journal of Electrochemical Science and Technology

Structuring of Bulk Silicon Particles for Lithium-Ion Battery Applications

Byoung Man Bang, Hyunjung Kim, and Soojin Park†
Interdisciplinary School of Green Energy, Ulsan National Institute of Science and Technology (UNIST), Ulsan 689-798, Korea

ABSTRACT :

We report a simple route for synthesizing multi-dimensional structured silicon anode materials from commercially available bulk silicon powders via metal-assisted chemical etching process. In the first step, silver catalyst was deposited onto the surface of bulk silicon via a galvanic displacement reaction. Next, the silver-decorated silicon particles were chemically etched in a mixture of hydrofluoric acid and hydrogen peroxide to make multi-dimensional silicon consisting of one-dimensional silicon nanowires and micro-scale silicon cores. As-synthesized silicon particles were coated with a carbon via thermal decomposition of acetylene gas. The carbon-coated multi-dimensional silicon anodes exhibited excellent electrochemical properties, including a high specific capacity (1800 mAh/g), a stable cycling retention (cycling retention of 89% after 20 cycles), and a high rate capability (71% at 3 C rate, compared to 0.1 C rate). This process is a simple and mass-productive (yield of 40-50%), thus opens up an effective route to make a high-performance silicon anode materials for lithium-ion batteries.

Keywords: Bulk silicon, Chemical etching, Structuring of silicon, Lithium ion battery

Received September 3, 2011 : Accepted September 17, 2011

1. Introduction

Conventional lithium-ion batteries (LIBs) have been widely used to information-based mobile electronic devices. However, the next generation of transportation, such as electric vehicle (EV), hybrid EV (HEV), and plug-in EV (PHEV), requires batteries with high energy and high power densities.[1)]

The most widely used anode materials are carbon-based materials, like natural graphite and mesocarbon microbead. However, the capacity of graphite is limited to 372 mAh/g. In contrast, anode materials (such as tin (Sn), antimony (Sb), silicon (Si), and germanium (Ge)) forming alloys with lithium are more attractive, since they can exhibit higher specific capacity. Among them, Si anode materials could significantly increase the energy density of LIBs. The Si has the highest theoretical gravimetric capacity (3580 mAh/g with formation of $Li_{15}Si_4$), a low average delithiation voltage (~0.4 V), and a large volumetric capacity (8340 mAh/cm^3).[2)] However, bulk Si anodes have one major problem that should be solved, i.e., a huge volume change of > 300% during Li insertion and extraction. The stress induced by the large volume change causes cracking and pulverization of the Si anode, leading to loss of electrical contact and eventual capacity fading.[3)]

To solve these problems, the concepts of nanostructured Si anodes have been extensive developed, including zero-dimensional (0D), 1D, 2D, and 3D Si materials.[4)] The nanomaterials showed significantly enhanced charge/discharge kinetics and increasing specific capacity in LIBs. However, the nanomaterials have some problems, like low thermodynamic stability, serious side reaction due to a high surface area, and high cost.[5,6)] Therefore,

†Corresponding author. Tel.: +82-52-217-2515
E-mail address: spark@unist.ac.kr

combining advantages of both micro- and nanomaterials is another strategy to develop high performance anode materials in LIBs. The micro-/nanoscale hybrid materials can be classified as follows: i) nanomaterials dispersed in a microscale matrix, ii) microscale active materials coated with nanostructured (inactive or active) materials, iii) mixtures of micro- and 1D nanomaterials.[7)]

Here, we demonstrate a synthesis of multi-dimensional bulk Si anodes that is composed of microscale Si matrix and 1D nanowires. Metal deposition onto the surface of bulk Si particles and subsequent metal-assisted catalytic etching lead to the formation of multi-dimensional Si structures. Easy processing by the microscale Si matrix and alleviation of volume change by the 1D nanostructures enabled us to make high performance anode materials, including a high reversible capacity (1800 mAh/g) and a stable cycling retention (89% after 20 cycles).

2. Experimental

Commercially available Si powder (30 μm) was purchased from Aldrich. 5 g Si powders were immersed in a solution of 3 mM silver nitrate ($AgNO_3$) and 5 M HF for 5 min to deposit Ag layers onto the Si surface. Immediately after rinsing, the Ag-deposited Si powder was immersed in an etchant consisting of 5 M HF and 1.5% H_2O_2 at 50°C for 2 hr to produce multi-dimensional Si particles. The H_2O_2 acts as an oxidant and enhances the etching rate of the Si particles. As-synthesized Si powders were immersed in a concentrated nitric acid at 50°C for 2 hr to remove Ag particles and followed by drying in a vacuum oven at 100°C for 6 hr to remove water completely. Subsequently, the multi-dimensional Si samples were coated by carbon by thermal decomposition of acetylene gas at 700°C for 30 min in quartz furnace.

The crystal structures of bulk and etched Si were investigated by X-ray diffractometer (XRD) on a Rigaku D/MAX. Raman spectra were recorded on a JASCO spectrometer (NRS-3000) to obtain the characteristics of carbon layers onto the Si surface. A He-Ne laser (632.8 nm) was used as the excitation source.

For the electrochemical properties of bulk and etched Si anodes, coin-type half cells (2016R) consisting of Si powders (the working electrode) and Li metal (counter-electrode) were prepared under an argon-filled glove box. The electrode was composed of Si active material (70 wt%), super P carbon black (15 wt%), and polyvinylidene fluoride (PVDF) binder (15 wt%). The electrolyte was $LiPF_6$ (1 M) with ethylene carbonate/diethylene carbonate/dimethyl carbonate (EC/DEC/DMC, 30 : 40 : 30 vol%). The coin cells were cycled at a rate of 0.1-3 C between 0.01 and 1.2 V.

3. Results and discussion

Electroless deposition can be applied to various systems, including metal-on-metal, metal-on-semiconductor, and metal-on-insulator. It is commonly classified into three different plating mechanisms, such as autocatalytic, substrate catalyzed, and galvanic displacement processes.[8)] In particular, the galvanic reaction can be carried out in the absence of an external reducing agent. Semiconductor, like Si and Ge, has been usually used, because it offers electrons to metal ions. In this manner, metal (e.g., Au, Ag, Cu, Pt) particles can be deposited onto the surface of Si.[9)]

We used commercially available bulk Si powders to make multi-dimensional Si anodes. Fig. 1 shows schematic illustration for synthesis of the multi-dimensional Si particles. Initially, the Si powders were immersed in a mixture of $AgNO_3$ and HF to deposit Ag nanoparticles

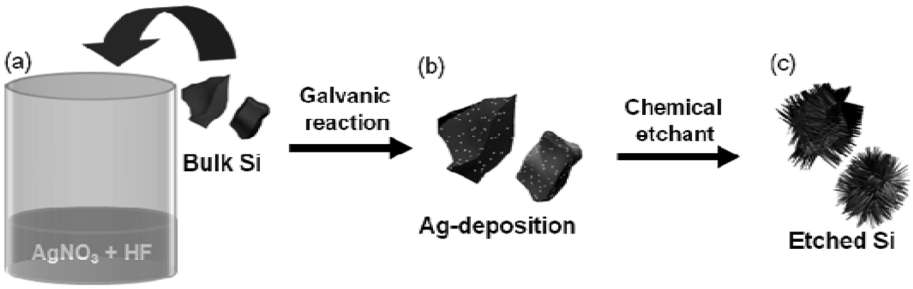

Fig. 1. Schematic illustration for synthesis of chemically etched Si powders. (a) Bulk Si powders have a broad size distribution of 2-40 μm. (b) When the Si was immersed in HF and $AgNO_3$ mixture, Ag nanoparticles were deposited onto the Si surface. (c) Immersion of Ag deposited Si in a chemical etchant (HF/H_2O_2) led to a formation of multi-dimensional Si particles having narrower size distribution of 10-15 μm.

onto the Si surface via galvanic displacement reaction (Fig. 1(b)). Subsequently, Ag deposited Si particles were chemically etched in an etchant consisting of HF and H_2O_2 at 50°C for 2 hr to make uniform-sized multi-dimensional Si particles (Fig. 1(c)). In the galvanic reaction, Ag nanoparticles act as a local cathode while the Si serves as an anode to form an electrochemical cell. The half cell reactions are described as follows:[10)]

Anode (Si)

$$Si + 2H_2O \rightarrow SiO_2 + 4H^+ + 4e^-$$

$$E^0 = 0.91 \text{ V (vs. SHE)} \quad (1)$$

$$SiO_2 + 6HF \rightarrow [SiF_6]^{2-} + 2H_2O + 2H^+ \quad (2)$$

Cathode (Ag)

$$H_2O_2 + 2H^+ + 2e^- \rightarrow 2H_2O$$

$$E^0 = 1.78 \text{ V (vs. SHE)} \quad (3)$$

The total reaction

$$Si + 2H_2O_2 + 6F^- + 4H^+ \rightarrow [SiF_6]^{2-} + 4H_2O \quad (4)$$

For the total reaction, the standard potential is 2.69 V, indicating that the etching process is thermodynamically favored. At the anode side, the Si is continuously dissolved by transferring electron to the upper surfaces of the Ag particles to reduce H_2O_2 into H_2O. At the cathode part, Ag particles can also be oxidized into Ag^+ by H_2O_2 according to the following reaction:

$$2Ag + H_2O_2 + 2H^+ \rightarrow 2Ag^+ + 2H_2O \quad (5)$$

The Ag^+ ions can be quickly reduced to Ag by taking electrons from Si before they can diffuse out according to the following reaction:

$$Si + 4Ag^+ + 6F^- \rightarrow 4Ag + SiF_6^{2-} \quad (6)$$

In this manner, the Ag particles are confined in the nanopits that formed during the galvanic reaction and the Si below the Ag particles is continuously etched down to make the Si nanowires.

Fig. 2 shows SEM images of as-synthesized multi-dimensional Si particles. When bulk Si powder was immersed in a solution of 3 mM $AgNO_3$ and 5 M HF for 5 min at room temperature, Ag nanoparticles with tens-of-nanometre size were prepared onto the Si surface via galvanic reaction (Fig. 2(a)). After rinsing excess amount of silver salts with a copious of deionized water for several times, the Ag deposited Si powder was put into an etchant consisting of 5 M HF and 1.5% H_2O_2 at 50°C for 2 hr. As-synthesized Si particles show multi-dimen-

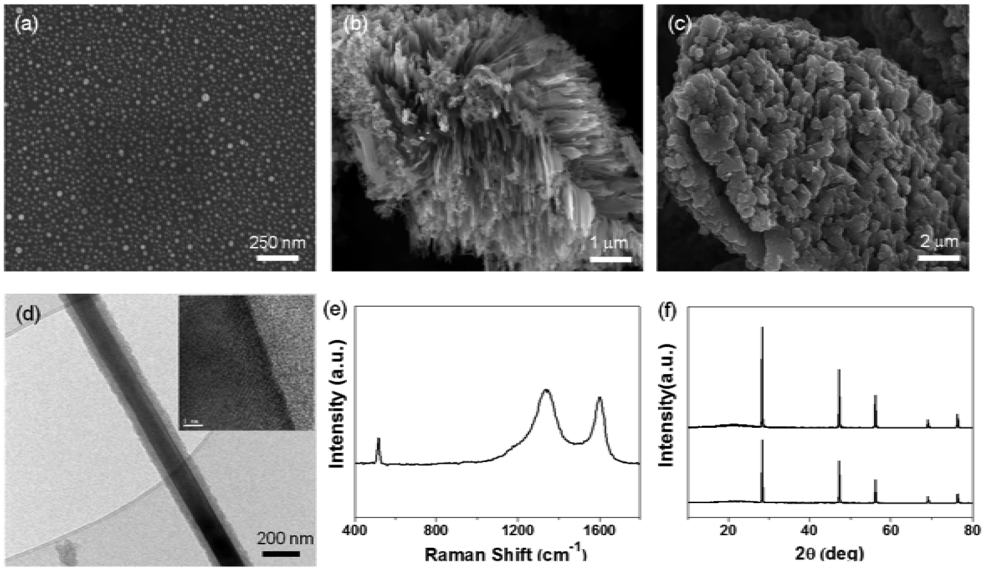

Fig. 2. Characterization of multi-dimensional Si structures. (a) Ag nanoparticles were deposited onto the Si surface via galvanic reaction. SEM images of chemically etched multi-dimensional Si (b) and carbon coated multi-dimensional Si (c) were seen. (d) TEM image of isolated Si nanowires shows a uniform carbon layer. Inset is a magnified TEM image showing a highly crystalline Si. (e) Raman spectrum shows an amorphous characteristic of carbon layer (I_D/I_G ratio = 2.1). (f) XRD patterns show a crystalline Si structure of the multi-dimensional silicon materials before and after carbon coating (top: before carbon coating, bottom: after carbon coating).

sional structures that Si nanowires (average length of 5 mm) protrude out from the Si surfaces (Fig. 2(b)). To investigate morphologies of Si nanowires, the multi-dimensional Si samples were dispersed in methanol and followed by ultrasonication for 5 min. The transmission electron microscope (TEM) image of Si nanowires transferred onto carbon-coated copper grids showed an average diameter of 100 nm (Fig. 2(d)), and the inset indicates a single crystalline characteristic of Si.

In order to use the chemically etched Si samples in LIBs, a carbon coating onto the Si surface should be carried out to enhance the poor electronic conductivity of Si. Various approaches, like chemical vapor deposition, pyrolysis, and mechanical milling, have been used.[11-14] We employed thermal decomposition process of acetylene gas that was performed at 700°C for 30 min in quartz furnace to coat the carbon layer onto the Si surface. At this time, carbon contents of 20 wt% were measured by inductively coupled plasma atomic emission spectroscopy analysis. The thermal decomposition process is effective method for filling the empty regions of etched Si particles. Since a thick carbon layer was coated onto the Si surface, the multi-dimensional Si structures were not clearly observed, but the carbon coating process did not destroy the multi-dimensional Si structures (Fig. 2(c)). Raman scattering of the carbon coated Si particles shows two peaks at ~1360 and ~1580 cm^{-1} correspond to the D (disordered) band and the G (graphene) band, respectively (Fig. 2(e)). The ratio of the D band to the G band was estimated to be 2.1, indicating an amorphous carbon characteristic.[15] Also, a peak of Si below the carbon layers was seen at 520 cm^{-1}. Before and after carbon coating, the morphology of chemically etched Si particles remains unchanged, and the XRD pattern indicates the same crystalline structure of Si (Fig. 2(f)).

Fig. 3(a) shows the voltage profiles of the multi-dimensional Si electrodes with a carbon content of 20 wt% at 0.1 C rate between 1.2 V and 0.01 V in a coin-type half cell. The first discharge and charge capacities are 2430 and 2150 mAh/g, respectively, indicating a coulombic efficiency of 87%. The high coulombic efficiency of the first cycle may be due to the uniform coating of the carbon layer, which can minimize the direct contact between the Si and electrolyte, and promotes the formation of

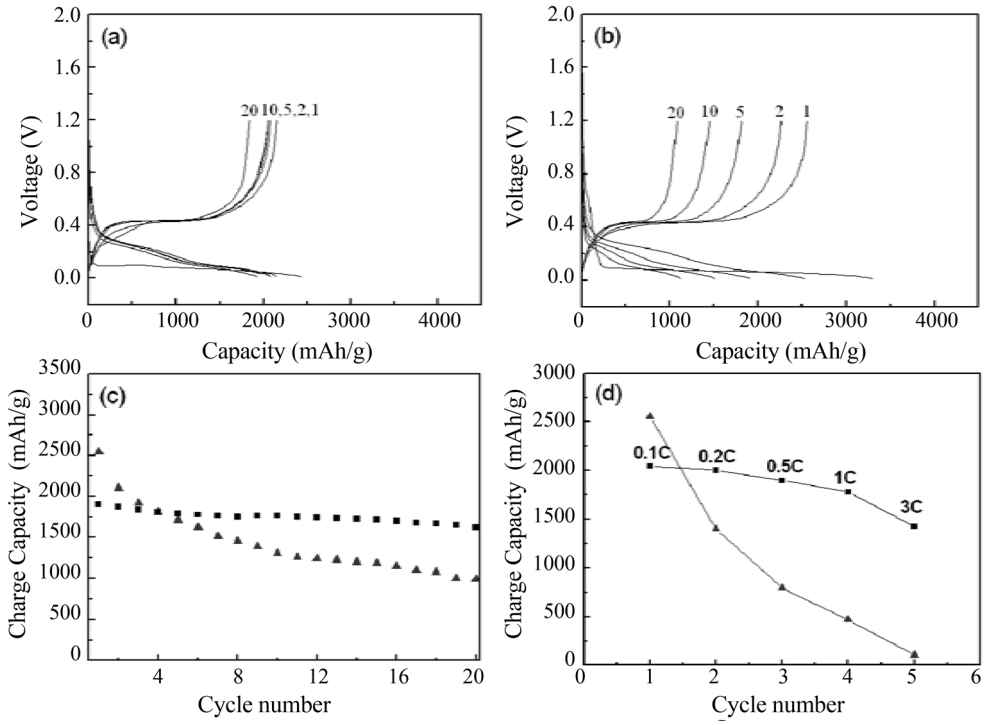

Fig. 3. Electrochemical properties for carbon-coated Si electrodes. Voltage profiles for the first, second, tenth, and twentieth galvanostatic cycles of the etched Si (a) and bulk Si (b) at a 0.1 C rate were seen. (c) Cycle retention of etched Si (square) and bulk Si (triangle) are seen. (d) Rate capabilities of etched Si (square) and bulk Si (triangle) were plotted.

the stable solid/electrolyte interface (SEI) layer on the surface of etched Si. Moreover, the morphology of multi-dimensional Si anode may enhance the accessibility of electrolytes and lithium ions, resulting in the significant improvement of the initial coulombic efficiency.

Since the 1D nanowires protruding out from the Si surface and the interstitial regions between the nanowires act as a buffer layer for the large volume change during cycling, they show excellent capacity retention, similar as those seen in other systems, like 3D porous structures, nanotubes, and hollow spheres (Fig. 3(c)).[16-18] On the contrary, the first discharge and charge capacities of bulk Si with the same carbon content are 3460 and 2500 mAh/g, respectively, corresponding to a low coulombic efficiency of 72% (Fig. 3(b)). Moreover, rapid capacity fading was observed, resulting in a reversible capacity of ~1000 mAh/g in the 20th cycle by pulverization due to a large volume change during Li insertion and extraction process, as expected (Fig. 3(c)).[3] In case of the multi-dimensional Si anode, a rate capability is superior to that of bulk Si electrode. Fig. 3(d) shows charge capacity at various C rates from 0.1 C to 3 C rate (discharge rate was fixed at 0.1 C) between 1.2 V and 0.1 V. Even at a high rate of 3 C, the capacity retention of 73% was seen compared to that of 0.1 C rate in the etched Si electrodes. When the Si-based materials were suitably designed, the electrochemical performances, including a high specific capacity, a stable cycling retention, and excellent rate capability, were significantly improved.

Fig. 4(a) shows the SEM image of the chemically etched Si particles after 20 cycles. As seen in the inset, the surface of cycled electrodes exhibits a similar morphology to that of the original Si electrode, except for the formation of SEI layers. Also, we confirmed the transformation of crystalline Si into amorphous Si after cycling. Fig. 4(b) shows the XRD patterns of the etched Si electrodes after 20 cycles. It has been reported that the original crystalline Si phase is transformed into amorphous Si after the initial cycle.[19] After 20 cycles, only copper peaks used as a current collector were seen, while crystalline Si peaks completely disappeared.

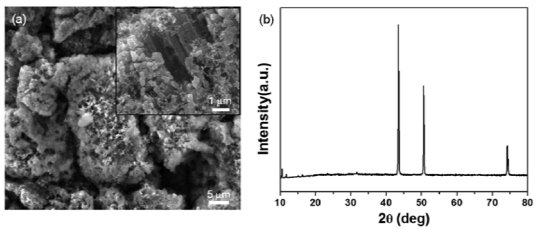

Fig. 4. Morphology of multi-dimensional Si electrodes after cycling. (a) SEM image of multi-dimensional Si electrodes after 20 cycles was seen. In the magnified SEM image, the pulverization of the Si nanowires was not observed. (b) XRD patterns of cycled Si electrodes indicated that only copper peaks used as current collector were seen, while crystalline Si peak disappeared due to the formation of amorphous Si.

4. Conclusions

We synthesized multi-dimensional silicon particles consisting of 1D Si nanowires and micro-scale Si cores from bulk Si powders via Ag-assisted chemical etching. This process is a simple and mass-productive (40-50% yield) to make high performance silicon anode materials. The multi-dimensional structures that are combined with 1D and 3D morphology accommodate large volume change during lithium insertion and extraction process. Therefore, they exhibited a high reversible capacity of ~1800 mAh/g with coulombic efficiency of 87% and stable cycle retention. This method may open up an effective way to make high performance anode materials in lithium ion batteries.

Acknowledgement

This research was supported by the MKE (The Ministry of Knowledge Economy), Korea, under the ITRC (Information Technology Research Center) support program supervised by the NIPA (National IT Industry Promotion Agency) (NIPA-2011-C1090-1100-0002).

References

1. J.-M. Tarascon and M. Armand, *Nature*, **414**, 359 (2001).
2. M. N. Obrovac and L. Christensen, *Electrochem. Solid-State Lett.*, **7**, A93 (2004).
3. U. Kasavajjula, C. Wang and A. J. Appleby, *J. Power Sources*, **163**, 1003 (2007).
4. M. G. Kim and J. Cho, *Adv. Funct. Mater.*, **19**, 1497 (2009).
5. P. G. Bruce, B. Scrosati and J.-M. Tarascon, *Angew. Chem. Int. Ed.*, **47**, 2930 (2008).
6. A. Manthiram, A. V. Murugan, A. Sarkar and T. Muraliganth, *Energy Environ. Sci.*, **1**, 621 (2008).
7. C. Liu, F. Li, L.-P. Ma and H.-M. Cheng, Adv. Mater., **22**, E28 (2010).
8. Y. Okinaka and M. Hoshino, *Gold Bull.*, **31**, 3 (1998).
9. G. Oskam, J. G. Long, A. Natarajan and P. C. Searson, *J. Phys. D*, **31**, 1927 (1998).
10. K. Q. Peng, A. J. Lu, R. Q. Zhang and S. T. Lee, *Adv. Funct. Mater.*, **18**, 3026 (2008).
11. A. M. Wilson, J. N. Reimers, E. W. Fuller and J. R.

Dahn, *Solid State Ionics*, **74**, 249 (1994).
12. C. S. Wang, G. T. Wu, X. B. Zhang, Z. F. Qi and W. Z. Li, *J. Electrochem. Soc.,* **145**, 2751 (1998).
13. Y.-S. Hu, R. Demir-Cakan, M.-M. Titirici, J.-O. Müller, R. Schlögl, M. Antonietti and J. Maier, *Angew. Chem. Int. Ed.,* **47**, 1645 (2008).
14. A. Magasinski, P. Dixon, B. Hertzberg, A. Kvit, J. Ayala and G. Yushin, *Nat. Mater.,* **9**, 353 (2010).
15. H. Lee and J. Cho, *Nano Lett.,***7**, 2638 (2007).
16. H. Kim, B. Han, J. Choo and J. Cho, *Angew. Chem. Int. Ed.,* **47**, 10151 (2008).
17. M.-H. Park, M. G. Kim, J. Joo, K. Kim, J. Kim, S. Ahn, Y. Cui and J. Cho, *Nano Lett.,* **9**, 3844 (2009).
18. H. Ma, F. Cheng, J.-Y. Chen, J.-Z. Zhao, C.-S. Li, Z.-L. Tao and J. Liang, *Adv. Mater.,* **19**, 4067 (2007).
19. Y.-M. Kang, J.-Y. Go, S.-M. Lee and W.-U. Choi, *Electrochem. Commun.,* **9**, 1276 (2007).